3D Printing and Mechanical Properties of Polyamide Products with Schwartz Primitive Topology

S. Balabanov, A. Makogon, M. Sychev, Alexei Evstratov, Arnaud Regazzi, José-Marie Lopez-Cuesta

▶ **To cite this version:**

S. Balabanov, A. Makogon, M. Sychev, Alexei Evstratov, Arnaud Regazzi, et al.. 3D Printing and Mechanical Properties of Polyamide Products with Schwartz Primitive Topology. Technical Physics / Zhurnal Tekhnicheskoi Fiziki, 2020, 65 (2), pp.211-215. 10.1134/S1063784220020036 . hal-02563219

HAL Id: hal-02563219

https://imt-mines-ales.hal.science/hal-02563219v1

Submitted on 25 May 2021

HAL is a multi-disciplinary open access archive for the deposit and dissemination of scientific research documents, whether they are published or not. The documents may come from teaching and research institutions in France or abroad, or from public or private research centers.

L'archive ouverte pluridisciplinaire **HAL**, est destinée au dépôt et à la diffusion de documents scientifiques de niveau recherche, publiés ou non, émanant des établissements d'enseignement et de recherche français ou étrangers, des laboratoires publics ou privés.

3D Printing and Mechanical Properties of Polyamide Products with Schwartz Primitive Topology

S. V. Balabanov[a,*], A. I. Makogon[a], M. M. Sychev[a,b], A. A. Evstratov[c], A. Regazzi[c], and J. M. Lopez-Cuesta[c]

[a] *Grebenshchikov Institute of Silicate Chemistry, Russian Academy of Sciences, St. Petersburg, 199034 Russia*

[b] *St. Petersburg State Technological Institute (Technical University), St. Petersburg, 190013 Russia*

[c] *IMT Mines Alès (EMA), Ales, 30319 France*

**e-mail: sergeybalabanov@yahoo.com*

Abstract—The results of a study of the mechanical properties of the honeycomb material made of polyamide-12, which consists of structural elements that repeat in three directions and have Schwartz primitive geometry, are presented. Samples in the form of a cube (size 30 × 30 × 30 mm) are obtained by layer-by-layer sintering of powder material on a 3D printer of selective laser sintering (SLS) type. Compression tests of samples with various geometry show that the strength of the samples increases with a decrease in the characteristic size of the repeating structural element. According to the calculations performed by the finite element method, this is caused by an increase in the dangerous sectional area. The possibility of a significant increase in the specific strength of the material while maintaining its density is shown.

INTRODUCTION

In this study, the mechanical properties of the cellular material made of polyamide-12, which consists of structural elements that repeat in three directions and has Schwartz primitive geometry, are studied. Cellular structures make it possible to optimize the ratio between the strength of a material and its weight. In [1, 2], academician V.Ya. Shevchenko expressed the idea of using similar objects with triple periodic minimal surface (TPMS) geometry for extreme loading conditions. The method of 3D printing is the most technologically advanced method for producing objects with such complex geometry [3, 4].

Objects that have the geometry of triply periodic minimal surface consist of repeating elements with the smallest possible area [5]. They combine surfaces with positive and negative curvature. Schwartz's primitive, i.e., infinite triply periodic structures (with periodicity along three axes), is an example of such surfaces (Fig. 1). The produced surface is described by the following rigorous mathematical equation, by means of which one can vary the geometry and, consequently, the properties of the obtained materials:

$$\cos(x) + \cos(y) + \cos(z) = t. \quad (1)$$

Due to the unique structure, materials that have the TPMS geometry represent composite materials composed of two mutually interpenetrating phases (in this case, one of the phases is air). Such objects have a number of interesting properties, including mechanical ones [6]. For example, materials with the TPMS geometry can efficiently dissipate the mechanical energy [7]. Thus, these kinds of materials can be used as components that absorb the energy of strikes and explosions, as a part of armor protection, or as a basis for energy-absorbing components of vehicles.

At present, there are practically no theoretical approaches that can predict the mechanical properties of such materials; therefore, the geometric parameters of a cellular honeycomb material with a Schwartz primitive structure have been experimentally optimized in this study to achieve the maximum strength and the ability to absorb shock energy.

The objective of this study was to produce materials with the TPMS geometry and to study their physicomechanical properties.

EXPERIMENTAL

At the first stage, 3D models of samples with Schwartz primitive topology with an various value of parameter t were created (Fig. 1). An increase in t leads to a decrease in the characteristic size of the repeating structural element. The 3D models were created using the Rhinoceros 6 software package for parametric modeling with the Grasshopper plugin and saved in the STL format used in 3D printing devices. The Autodesk Netfabb software was used to fix errors in the

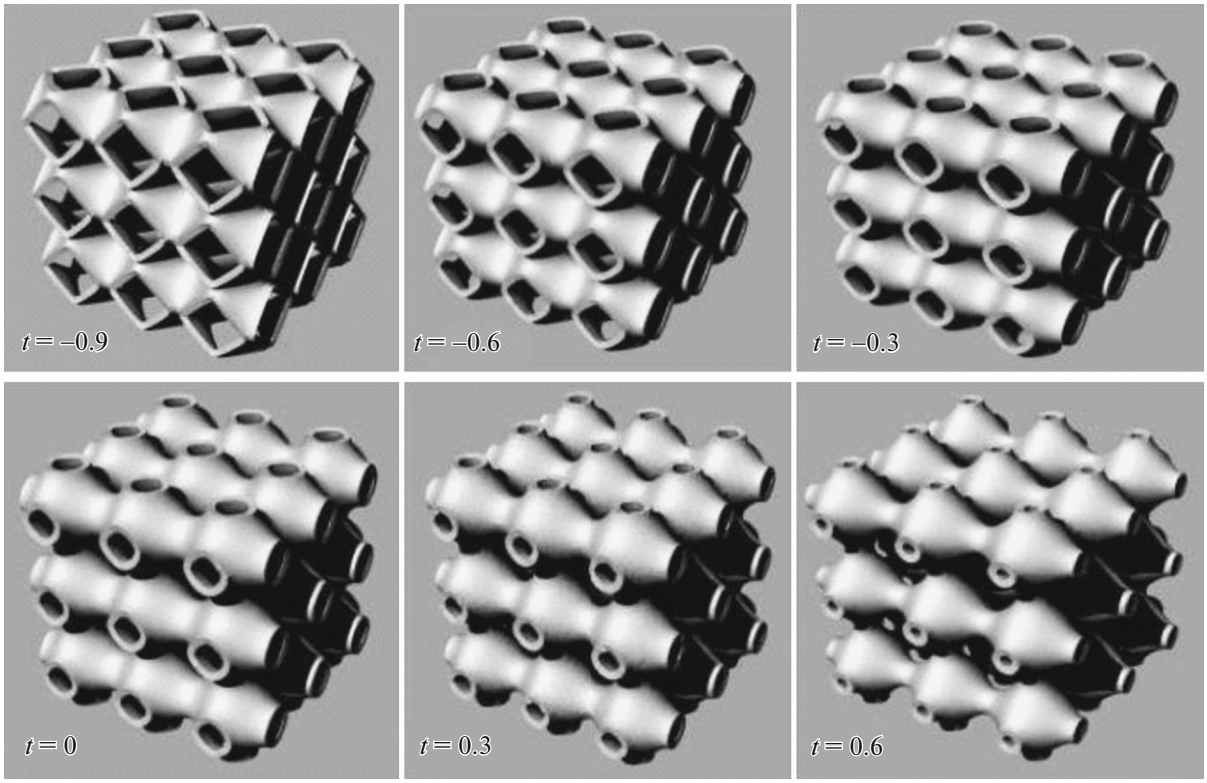

Fig. 1. Changes in the geometry of the samples as a function of parameter t in Eq. (1).

STL files. To prepare models for SLS printing, the EOS Parameter Editor module was used.

Based on the created 3D models, samples were prepared by selective laser sintering (SLS technology) on a 3D printer from EOS (model FORMIGA P110).

Selective laser sintering is an additive manufacturing method used to create functional prototypes and small batches of finished products. The technology is based on sequential sintering of layers of a powder material by high-power lasers. The printing conditions are as follows: the layer height is 100 μm, the temperature of the stage is 169.5°C, and the temperature of the chamber is 150°C. After printing, the samples were cleaned of the remains of unsintered powder by processing in a sandblasting apparatus.

Polyamide-12 (PA2200 brand) was used as a printing material. Polyamide-12 is a product of polymerization of dodecalactam, representing a structural crystallizing material with increased elasticity. The melting temperature of unfilled grades is 173–180°C. The glass transition temperature is 35–37°C. The degree of crystallinity is 40–70%. It is characterized by high resistance to cracking and high wear resistance and has low moisture absorption, high dimensional stability, and good dielectric properties [8].

The produced samples consist of 27 unit cells (Fig. 1). The wall thickness of the samples is 0.8 mm. The sample dimensions are 30 × 30 × 30 mm. To study the mechanical properties, the samples were tested for compressive strength in accordance with International *Standart ISO 604:2002* on an Walter + Bai electromechanical testing machine with a maximum possible load of up to 400 kN at an air temperature of 26°C with a loading speed of 5 mm/min [9]. It is known, the mechanical properties of products made by 3D printing depend on the direction of loading [10]; therefore, the strength tests of all samples were carried out in the direction of growing the samples (along the Z axis).

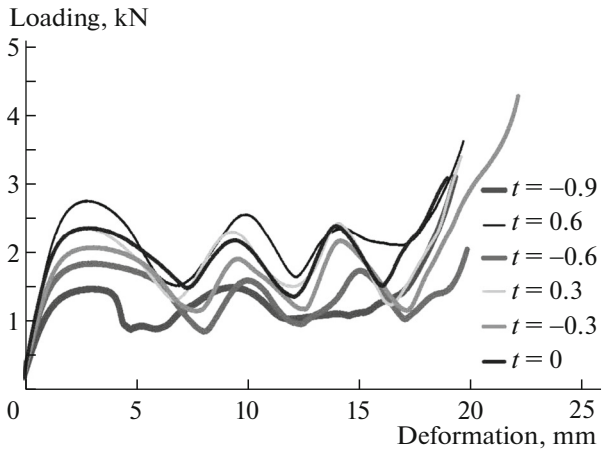

Fig. 2. Stress–strain curves.

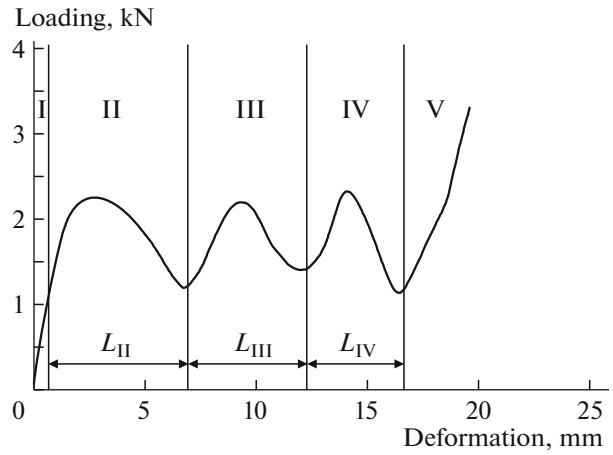

Fig. 3. Analysis of a stress–strain curve.

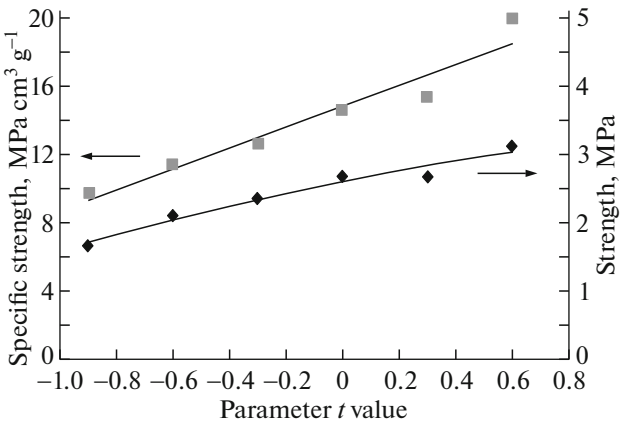

Fig. 4. Strength of the samples as a function of their geometry.

The mechanical properties of the samples were simulated using the finite element method in the COMSOL Multiphysics software package. The finite element method is a numerical method for solving differential equations with partial derivatives, as well as integral equations that arise when solving problems of applied physics. The method is widely used to solve problems of the mechanics of a deformable solid, as well as heat-transfer, hydrodynamics, and electrodynamics problems [11].

RESULTS AND DISCUSSION

The behavior of polymer materials subjected to forced elastic deformations is usually analyzed by means of compression curves (stress–strain curves). The stress–strain curves obtained in sample tests have their own specificity determined by complex geometry. Mechanical tests of the samples eventually give the dependences of the applied load on the degree of deformation (Fig. 2). In accordance with *Standart ISO 604:2002*, the first peak on the stress–strain curve, which corresponds to the transition of the sample to the region of plastic deformation, was taken as the sample strength. The curves have three pronounced extrema (peaks), each of which corresponds to the destruction of a cell layer that lies in a plane perpendicular to the axis of loading.

To analyze the stress–strain curve, it is convenient to divide it into typical sections. We divided the stress–strain curves into five sections (Fig. 3).

Section I is characterized by the fact that the stress sharply increases with deformation of the sample. The law of proportionality (Hooke's law) is satisfied in this section. This is a section of elastic deformation; at the end of section I, Hooke's law is no longer valid. Next, three elastoplastic deformation sections are observed, which are mutually similar to each other. There is a maximum in section II; at the extremum point, the first layer of cells begins to rapidly deform. Further, the stress drops with a rapid increase in the strain. At the end of section II and the beginning of section III, the first layer of cells completely collapses. Sections III and IV essentially repeat section II, but one can note that the lengths of sections L_{II}, L_{III}, and L_{IV} (degree of deformation) are successively decreasing in the order of $L_{II} > L_{III} > L_{IV}$. At the end of IV and the beginning of section V, the third layer of cells completely collapses. In section V, an exponential increase in the load begins; this is a section of plastic deformation.

The position of the maximum points on the curve depends on a number of factors, such as the structure of the polymer, its molecular weight, temperature, compression rate, load conditions, etc. The number of peaks (maxima) on the stress–strain curve corresponds to the number of cell layers aligned perpendicular to the axis of loading.

As follows from the analysis of the stress–strain curves, the sample strength increases almost linearly

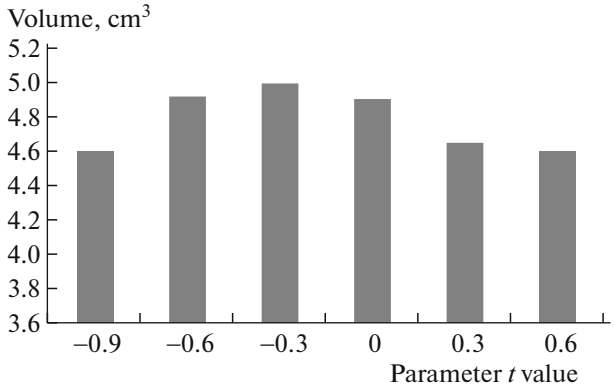

Fig. 5. Volume of the samples as a function of the parameter t.

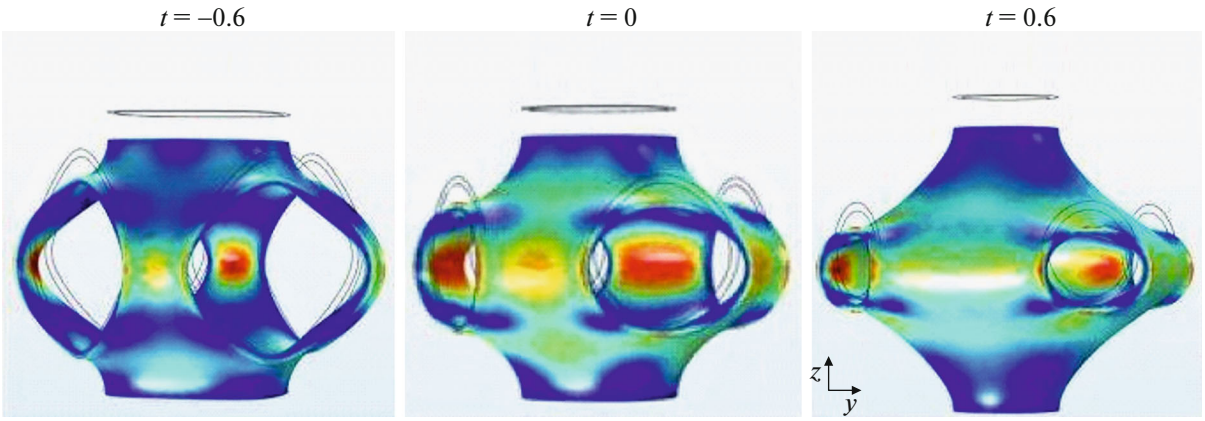

Fig. 6. Stress distribution in unit cells of the samples.

with an increase in parameter t (Fig. 4). Moreover, the sample volume nonlinearly depends on t (Fig. 5). Therefore, the dependence of the specific strength on parameter t is somewhat different from the corresponding dependence for the strength, namely: a linear increase of the specific strength is observed with an increase in t (Fig. 4).

According to the results of computer simulation by the COMSOL Multiphysics software, mechanical stresses are unevenly distributed throughout the sample when a compressive load is applied (Fig. 6). The magnitude of mechanical stresses reaches the highest values in the central sections of the cells. In these areas the structures have the lowest strength. These calculations are confirmed by experimental data. A visual inspection of the samples after testing revealed cracks (Fig. 7) precisely in the regions corresponding to the maximum load found from the calculation data (Fig. 6).

With an increase in parameter t, the area of the unsafe section increases (Fig. 8). On account of this, the stresses in the unsafe section are reduced and the sample strength increases.

It should be noted that the density of the studied samples is 5–6 times lower than that of monolithic samples of the same material.

According to [12], the cellular elements have a low density and a high strain under a load, matching the properties of a plastic material [8]:

(i) $\rho_1 = 0.38$ g/cm^3, $\sigma_1 \approx 6$ MPa, $\varepsilon_{\text{lim }1} \approx 55\%$, $\sigma_{\text{spec }1} \approx 15.8$ MPa cm^3 g^{-1};

(ii) $\rho_2 = 0.73$ g/cm^3, $\sigma_2 \approx 6$ MPa, $\varepsilon_{\text{lim }2} \approx 28\%$, $\sigma_{\text{spec }2} \approx 17.8$ MPa cm^3 g^{-1}.

Thus, the optimization of the geometry of the material with the TPMS structure made it possible to achieve a specific strength of 20 MPa cm^3 g^{-1} with a density of 0.16 g/cm^3; this is superior to both classical honeycomb structures [12] and the results shown in the publication [7].

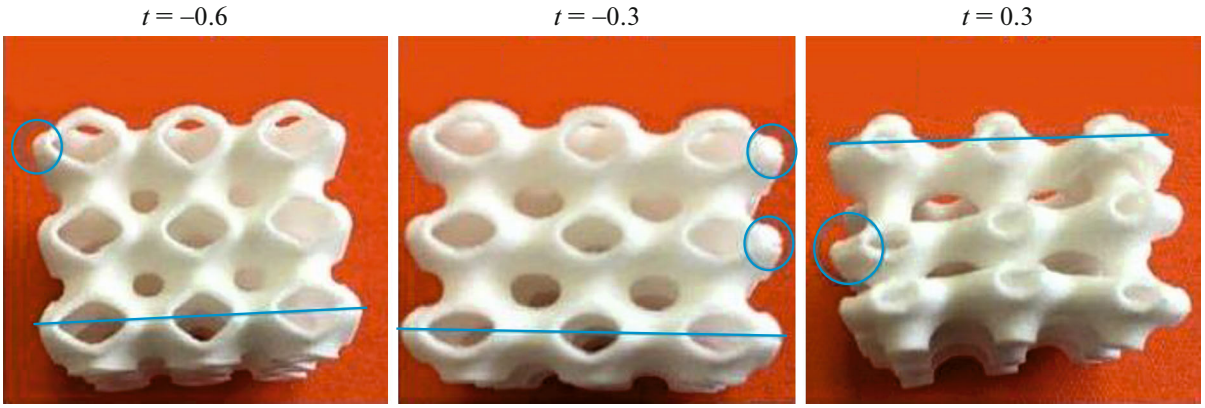

Fig. 7. Samples after testing. Circles show the sites with emerging cracks.

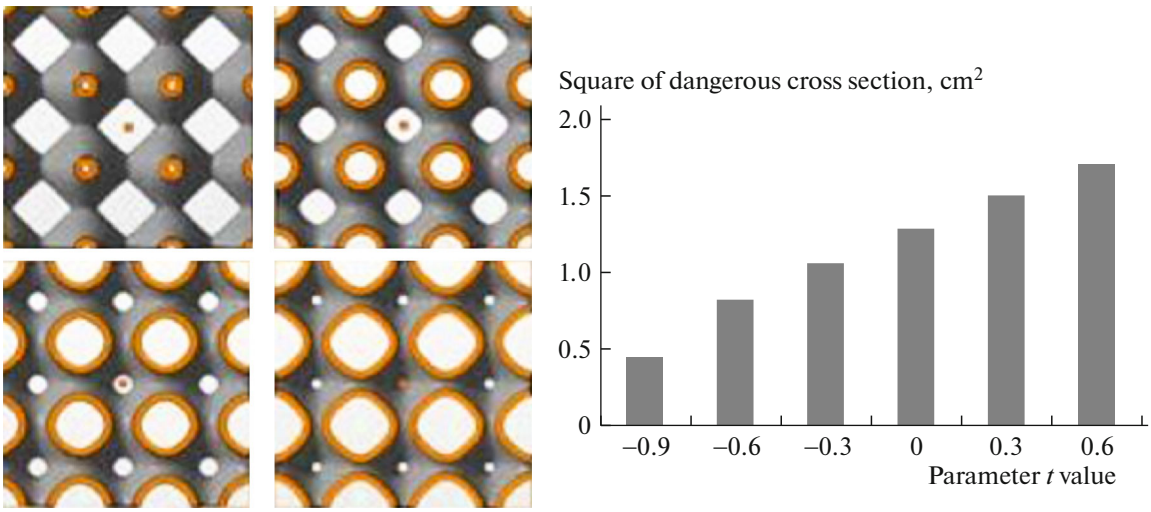

Fig. 8. Change in the area of the unsafe section as a function of parameter *t*.

CONCLUSIONS

1. Using the SLS method of 3D printing, samples with Schwartz's primitive topology of a triple periodic minimum surface with different values of parameter *t* are obtained.

2. It is found that the specific strength of the samples increases by a factor of 2 from 10 to 20 MPa $cm^3 g^{-1}$ with an increase in *t*. This is due to the fact that the area of the unsafe section increases with an increase in parameter *t* (Fig. 8), a consequence of which is the stresses in the unsafe section decrease and the sample strength increases.

3. The optimization of the geometry of the material with the TPMS structure makes it possible to achieve a specific strength of 20 MPa $cm^3 g^{-1}$ with a density of 0.16 g/cm^3, which is superior to classical honeycomb structures.

4. The density of TPMS samples of Schwartz primitive type is 5–6 times lower than that of solid cast samples of the same material, which means that the weight of such products will be lower with the same size and shape, allowing one to use the developed materials with a periodic structure as energy-absorbing structural components of sea and river vessels, spaceships, and aircrafts, and in the automotive industry.

ACKNOWLEDGMENTS

We are grateful to L.A. Lebedev and S.V. D'yachenko for their help in conducting mechanical tests during this study.

FUNDING

The study was supported by a grant from the Russian Science Foundation (project no. 17-13-01382).

CONFLICT OF INTEREST

The authors declare that they do not have any conflicts of interest.

REFERENCES

1. V. Ya. Shevchenko, M. M. Sychev, A. E. Lapshin, and L. A. Lebedev, Glass Phys. Chem. **43**, 605 (2017).
2. V. Ya. Shevchenko, M. M. Sychev, A. E. Lapshin, L. A. Lebedev, A. A. Gruzdkov, and A. M. Glezer, Glass Phys. Chem. **43**, 608 (2017).
3. D. W. Abueidda, M. Bakir, R. K. Abu Al-Rub, J. S. Bergstrom, N. A. Sobh, and I. Jasiuk, Mater. Des. **122**, 255 (2017).
4. D. W. Abueidda, M. Elhebeary, C.-S. Shiang, S. Pang, R. K. Abu Al-Rub, and I. Jasiuk, Mater. Des. **165**, 107597 (2019).
5. E. A. Lord, A. L. Mackay, and S. Ranganathan, *New Geometries for New Materials* (Cambridge Univ. Press, 2006).
6. J. Qu, M. Kadic, A. Naber, and M. Wegener, Sci. Rep. **7**, 40643 (2016).
7. M. Sychov, L. Lebedev, S. V. Dyachenko, and L. A. Nefedova, Acta Astronaut. **150**, 81 (2018).
8. W. Griehl and D. Ruestem, Ind. Eng. Chem. **62**, 16 (1970).
9. *GOST 4651–2014 (ISO 604:2002): Plastics. Compression Test Method* (Standartinform, Moscow, 2014).
10. S. V. D'yachenko, L. A. Lebedev, M. M. Sychev, and L. A. Nefedova, Tech. Phys. **63**, 984 (2018).
11. O. C. Zienkiewicz, *The Finite Element Method in Engineering Science,* 2nd ed. (McGraw-Hill, 1971).
12. V. A. Markov, V. I. Pusev, and V. V. Selivanov, Vopr. Oboronnoi Tekh., Nos. 7–8, 54 (2012).

Translated by O. Kadkin